Journal of Solid State Chemistry **153,** 74–81 (2000)
doi:10.1006/jssc.2000.8749, available online at http://www.idealibrary.com on IDEAL®

Characterization of the Nickel Cobaltite, $NiCo_2O_4$, Prepared by Several Methods: An XRD, XANES, EXAFS, and XPS Study

J. F. Marco,[1] J. R. Gancedo, and M. Gracia

Instituto de Química-Física "Rocasolano," CSIC, c/Serrano, 119, 28006 Madrid, Spain

J. L. Gautier[1] and E. Ríos

Facultad de Química y Biología, Universidad de Santiago de Chile, c.c. 40, Santiago 33, Chile

and

F. J. Berry

Department of Chemistry, The Open University, Walton Hall, Milton Keynes MK7 6AA, England

Received January 26, 2000; in revised form April 7, 2000; accepted April 20, 2000; published online July 7, 2000

The bulk structural properties of the nickel cobaltite, $NiCo_2O_4$, prepared by the thermal decomposition of carbonates, sol–gel methods, and the decomposition of hydroxides, have been examined by X-ray powder diffraction (XRD) and X-ray absorption spectroscopy (EXAFS and XANES). The results indicate, as expected, that Ni occupies the octahedral sites of the spinel structure while Co occupies both tetrahedral and octahedral sites. The XANES and EXAFS data are compatible with the existence of Ni^{2+} and Ni^{3+}. The structural data indicate that Co is present as Co^{2+} and Co^{3+}.The bulk cation distribution appears to be dependent on the synthesis procedure. The results of the surface examination by X-ray photoelectron spectroscopy (XPS) show that the surface composition is different from the nominal bulk composition and also varies with the preparative method. All the XP spectra indicate the presence of Ni^{2+} and Ni^{3+}, their relative concentrations being noticeably dependent upon the synthesis method used. In contrast, the Co XP spectra recorded from all samples are very similar and indicate the presence of both Co^{2+} and Co^{3+}.

Key Words: **$NiCo_2O_4$; thermal decomposition of carbonates; sol–gel; decomposition of hydroxides; XRD; EXAFS; XANES; XPS.**

1. INTRODUCTION

The nickel cobaltite, $NiCo_2O_4$, has long been known to be an active bifunctional catalyst for oxygen evolution (1–3) and reduction in alkaline media (4, 5), and to be an effective electrode for organic electrosynthesis (6). Since the electrocatalytical properties of metal oxides can vary widely according to their method of preparation (7), it would be reasonable to expect that different preparative methods might yield forms of $NiCo_2O_4$ with significant differences both in the bulk and/or in the surface structure. For example, it has been recently shown (8) that the surface composition of $NiCo_2O_4$ prepared by thermal decomposition of nitrates in isopropanol solutions exhibits a strong enrichment in Ni.

$NiCo_2O_4$ reportedly adopts a pure spinel structure in which all the Ni ions occupy the octahedral sites and the Co ions are distributed among the tetrahedral and octahedral sites of the structure (9). The distribution of the cationic oxidation states is the matter of some uncertainty (10) and appears to reflect the type of characterization technique used and the method of synthesis of $NiCo_2O_4$.

We report here on the use of X-ray powder diffraction (XRD), X-ray absorption spectroscopy (EXAFS and XANES), and X-ray photoelectron spectroscopy (XPS) to determine the influence of the preparative method on the bulk and surface structure of $NiCo_2O_4$.

2. EXPERIMENTAL

2.1. Synthesis

$NiCo_2O_4$ was prepared by three different methods: by the thermal decomposition of carbonates, by sol–gel methods, and by the decomposition of hydroxides.

[1]To whom correspondence should be addressed.
Dr. J. F. Marco: Fax: 34.91.5642431, E-mail: jfmarco@iqfr.csic.es.
Dr. J. L. Gautier: E-mail: jgautier@lauca.usach.cl.

0022-4596/00 $35.00

(*a*) *Thermal decomposition of carbonates* (*CS*). The method was similar to that used previously (11). Stoichiometric amounts of commercial $CoCO_3$ and $NiCO_3 \cdot 2Ni(OH)_2 \cdot 4H_2O$ were thoroughly mixed in an agate mortar. The mixture was heated in flowing oxygen at 330°C for 24 h.

(*b*) *Sol–gel* (*SG*). A method similar to that used to prepare Co_3O_4 (12) and other Ni-containing spinels (13) was employed. Cobalt carbonate, $CoCO_3$, was freshly prepared by addition of sodium carbonate to a concentrated aqueous solution of cobalt chloride at 60°C. The precipitate was filtered, washed with hot water, and dried at 100°C. The fresh $CoCO_3$ powder was mixed with a stoichiometric amount of nickel carbonate and dissolved in excess propionic acid. The solution was heated at 140°C to evaporate the excess propionic acid and form a gel. Liquid nitrogen was added immediately to give a mixed nickel–cobalt propionate. This was subsequently heated at 200°C for 2 h to remove the excess propionic acid. The product was finally grounded at 325 mesh and calcined in air at 350°C for 24 h.

(*c*) *Thermal decomposition of hydroxides* (*COH*). A method similar to that used (14, 15) for the synthesis of $MnCo_2O_4$ was adopted. Stoichiometric aqueous solutions of cobalt and nickel nitrate were mixed and 1 M KOH was added dropwise under bubbling Ar to avoid carbonation. The precipitate was separated by centrifugation, washed with hot (60°C) distilled water, and dried at 130°C for 24 h. The ground solid was heated in air at 320°C for 24 h.

2.2. Characterization

X-ray powder diffraction patterns were recorded with a Philips 1050-80 diffractometer using Cu$K\alpha$ radiation ($\lambda = 1.54056$ Å) and a graphite monochromator. A 99.99% pure Si internal standard was used.

XANES and EXAFS measurements were performed on station 7.1 at the Synchrotron Radiation Source at Daresbury Laboratory operating at an energy of 2.0 GeV and an average current of 200 mA. Data were collected at 298 K using an Si(111) double crystal order sorting monochromator in transmission mode using 20% harmonic rejection. The energy scale was calibrated using a 6-μm Ni foil in the case of the Ni K-edge and a 6-μm Co foil for the Co K-edge. The position of the first inflection point on the Ni foil edge was taken at 8332.8 eV and that of the Co foil edge was at 7708.9 eV. All the Ni and Co XANES data reported here are referred to these two values. All the edges were recorded at least twice and at different times separated by several hours but within the lifetime of the beam. The reproducibility in the determination of the edge positions was found to be better than 0.2 eV. The edge profiles were separated from the EXAFS data and, after subtraction of the linear pre-edge background, normalized to the edge step. The positions of the edge maxima were obtained from the zeros of the first derivative of the edge profile and the position of the edges themselves was taken at the energy at which the normalized absorption was 0.5 (i.e., the absorption at half-height of the edge step). The EXAFS oscillations were isolated after background subtraction of the raw data using the Daresbury program EXBACK and converted into k space. The data were weighted by k^3, where k is the photoelectron wave vector, to compensate for the diminishing amplitude of the EXAFS at high k. The data were fitted using the nonlinear squares minimization program EXCURV90 (16) which calculates the theoretical function using the fast curved wave theory (17). The phase shifts were calculated from *ab initio* methods as described elsewhere (18) and tested on NiO and CoO, the results being in reasonable agreement with the published crystallographic data (differences in first-shell distances were less than 0.02 Å) (19, 20). The quality of the fit to the data was assessed by using statistical tests (21) and found to be significant at the 1% level.

XPS data were recorded with a triple channeltron CLAM2 analyzer under a vacuum better than 1×10^{-8} Torr using Al$K\alpha$ radiation and a constant analyzer transmission energy of 20 eV. All the spectra were recorded at a take-off angle of 90°. All binding energy values were charge corrected to the C 1*s* signal (284.6 eV). All the spectra were computer fitted using a program based on procedures described in the literature (22) and the binding energies are accurate to ± 0.2 eV. Relative atomic concentrations were calculated using tabulated atomic sensitivity factors (23).

3. RESULTS AND DISCUSSION

3.1. Bulk Characterization

All the compounds were found by XRD to be single phase with a spinel-related structure. The cubic lattice parameter a showed slight variations with the synthesis procedure (Table 1).

The Ni K-edge XANES of the products obtained by the three different synthesis methods are depicted in Fig. 1. The XANES recorded from an Ni foil and NiO are also shown. The absence in the XANES of well-defined pre-edge features precludes the existence of Ni ions in the tetrahedral sites of the spinel structure and indicates, in good agreement with the findings of other workers (10), that Ni ions in $NiCo_2O_4$ occupy only octahedral sites. Table 2 collects the edge positions of the $NiCo_2O_4$ materials made by the three methods and the shifts in the positions of the edges with respect to that of Ni metal. In the case of Ni it is known (24) that an increase of a unit in the oxidation state is reflected in a shift of ca. 1.5 eV in the position of the absorption edge. According to this, and the results shown in Fig. 1 and

TABLE 1
Cubic Lattice Parameters Calculated from the XRD Data

Synthesis procedure	Lattice parameter, a (Å)
$NiCo_2O_4$ (CS)	8.066(2)
$NiCo_2O_4$ (SG)	8.104(3)
$NiCo_2O_4$ (COH)	8.117(6)

TABLE 2
Ni K-Edge Positions

Sample	Edge position (eV)	Δ^a (eV)	Edge maximum (eV)
Ni	8332.8	—	—
NiO	8336.2	3.4	8343.0
$NiCo_2O_4$ (CS)	8336.8	4.0	8343.2
$NiCo_2O_4$ (SG)	8337.4	4.6	8344.2
$NiCo_2O_4$ (COH)	8337.6	4.8	8344.8

[a]Δ is the energy difference between the position of the edge in the compound and that of Ni metal.

Table 2, it becomes apparent that the average oxidation state of Ni in all the examined materials is higher than 2+. The compound made by thermal decomposition of carbonates has an edge position which is the closest to that of NiO. Thus, it seems reasonable to assume that this material has to contain the largest Ni^{2+} concentration in the three samples of $NiCo_2O_4$ made during this work. The edge shifts for the other two samples of $NiCo_2O_4$ are compatible with the presence of a large concentration of Ni^{3+}.

As a first crude approach the Ni K-edge EXAFS were fitted according to the crystallographic model proposed by Knop *et al.* (9), i.e., considering one first coordination shell of six oxygen atoms surrounding the central Ni atom and two further Ni and Co shells (composed of six atoms each) at longer distances. The results of such a fit are shown in Table 3. Considering that typical Ni^{2+}–O and Ni^{3+}–O distances in octahedral coordination are around 2.05–2.09 Å and 1.95–1.98 Å, respectively, the fit of the EXAFS data is consistent with the XANES observations in that it indicates the existence of the simultaneous presence of Ni^{2+} and Ni^{3+}. Thus, the longest Ni–O distance is obtained for the material prepared by the thermal decomposition of carbonates, suggesting that it contains the highest Ni^{2+} concentration. The Ni–O distances obtained in the $NiCo_2O_4$ prepared by sol–gel techniques and by the decomposition of hydroxides are shorter and thus compatible with major Ni^{3+} content.

In order to separate the contributions of the different oxidation states we adopted a second model to fit the EXAFS data which takes into account the existence of a longer Ni–O distance at around 2.05–2.09 Å, characteristic of Ni^{2+}, and a shorter Ni–O distance at 1.95–1.98 Å, characteristic of Ni^{3+}. This approach has also been used in the past (10). The ratio of the coordination numbers for each distance can be used to estimate the ratio of the different Ni oxidation states. However, an inherent problem in EXAFS data analysis is the difficulty of determining coordination numbers to a high degree of accuracy. This is chiefly because a strong correlation exists between the coordination numbers of each shell and its associated Debye–Waller factor, which is a measure of the thermal and/or static disorder of the atoms in the shell. During the initial analysis of the data, approximate values for coordination numbers were obtained by allowing the occupancies and Debye–Waller factors to refine. The coordination numbers were then allowed to refine separately and the final value was approximated to the nearest integer number. The results of this type of fit are

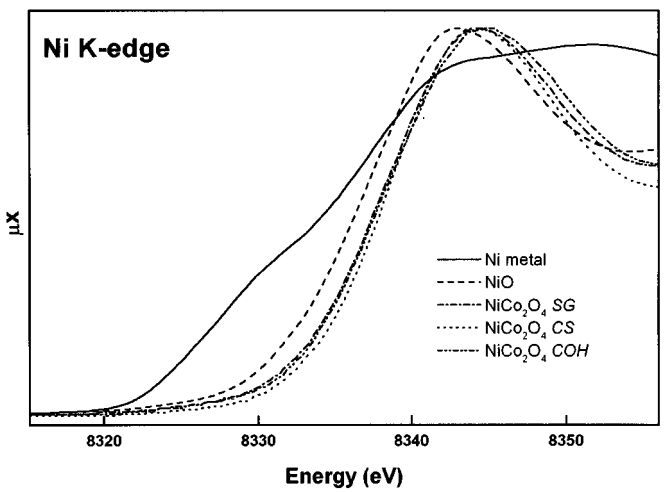

FIG. 1. Ni K-edge XANES.

TABLE 3
Final Fitting Parameters Obtained from the Fit of the Ni K-Edge EXAFS According to (9) and Considering a Single First Ni–O Shell

Sample	Atom type	Coordination number	Distance (Å)	$2\sigma^2$ (Å^2)
$NiCo_2O_4$ (CS)	O	6	2.02	0.016
	Ni	6	2.82	0.026
	Co	6	2.94	0.009
$NiCo_2O_4$ (SG)	O	6	1.99	0.018
	Ni	6	2.80	0.021
	Co	6	2.92	0.010
$NiCo_2O_4$ (COH)	O	6	1.96	0.018
	Ni	6	2.75	0.032
	Co	6	2.89	0.017

TABLE 4
Final Fitting Parameters Obtained from the Fit of the Ni K-Edge EXAFS Considering Two First Ni–O Shells

Sample	Atom type	Coordination number	Distance (Å)	$2\sigma^2$ (Å^2)
$NiCo_2O_4$ (CS)	O	5	1.94	0.016
	O	3	2.08	0.004
	Ni	6	2.79	0.023
	Co	6	2.94	0.007
$NiCo_2O_4$ (SG)	O	6	1.96	0.019
	O	2	2.09	0.012
	Ni	6	2.78	0.009
	Co	6	2.93	0.009
$NiCo_2O_4$ (COH)	O	6	1.95	0.018
	O	1	2.08	0.016
	Ni	6	2.75	0.032
	Co	6	2.89	0.017

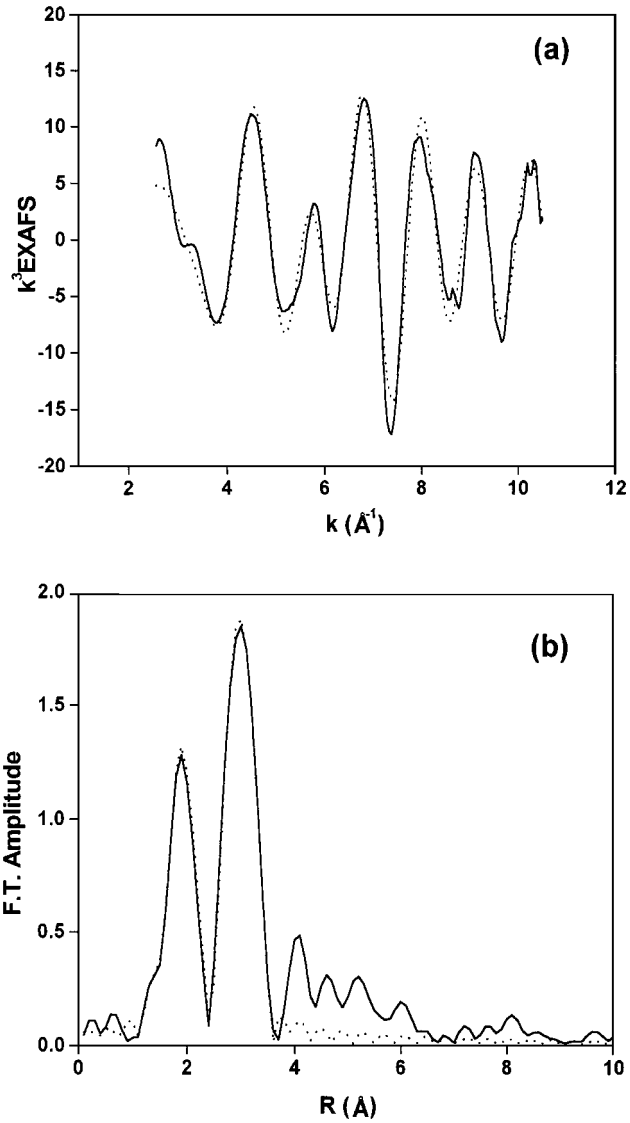

FIG. 2. (a) Ni K-edge EXAFS of $NiCo_2O_4$ prepared by the sol–gel method and (b) its corresponding Fourier transform (solid curve, experiment; dashed curve, fitted curve).

presented in Table 4 and we should comment that the quality of this fit was significantly better than that using only a single distance. We would like to comment that our treatment of the EXAFS data assumes simple regular octahedral environments for both Ni^{2+} and Ni^{3+} and does not take into account the possible Jahn–Teller distortion on the Ni^{3+} site (d^7 configuration). The consideration of Jahn–Teller distortion would imply the splitting of the single Ni^{3+}–O distance in the first coordination shell into at least two Ni^{3+}–O distances to account for such distortion. Consequently, two coordination numbers associated with both Ni^{3+}–O distances should be also introduced in the fitting procedure. The existence of two different oxidation states of Ni and the difficulties in determining accurately coordination numbers in EXAFS are serious limitations to elucidate in such a detail the structure of the octahedral sites. Thus, we prefer to adopt the model involving two distances which enables the determination of Ni^{2+}/Ni^{3+} ratios which are compatible with the XANES data.

Figure 2 shows the Ni K-edge EXAFS and Fourier transform for $NiCo_2O_4$ prepared by the sol–gel method. The best fit to the data recorded from $NiCo_2O_4$ made by the thermal decomposition of carbonates yields three oxygen atoms at 2.08 Å and five oxygen atoms at 1.94 Å. According to the obtained occupation numbers, the Ni^{2+}/Ni^{3+} ratio would be 0.6. In the case of the material made by sol–gel methods the results indicated the existence of six oxygen atoms at 1.96 Å and two oxygen atoms at 2.09 Å. The ratio Ni^{2+}/Ni^{3+} would be 0.33. The fit of the EXAFS for the material made by the decomposition of hydroxides yielded six oxygen atoms at 1.95 Å and one oxygen atom at 2.08 Å. In the latter case the Ni^{2+}/Ni^{3+} ratio decreased to 0.17.

Hence, in summary, the Ni K-edge XANES and EXAFS data indicate that the oxidation state of Ni in $NiCo_2O_4$ depends on the method of preparation with the Ni^{2+} content decreasing in the order CS > SG > COH.

The Co K-edge XANES recorded from the three compounds are depicted in Fig. 3 together with the XANES recorded from a Co foil and from CoO. The edge positions of the three samples of $NiCo_2O_4$ and the shifts in the positions of the edges with respect to that of Co metal are collected in Table 5. In all cases the edge position of the nickel cobaltites appears at a higher energy than that of CoO, indicating that all the compounds contain both Co^{2+} and Co^{3+}. The broad pre-edge feature observed in the XANES, which extends over ca. 6 eV, is due to the superposition of the component corresponding to the $1s \rightarrow 3d$

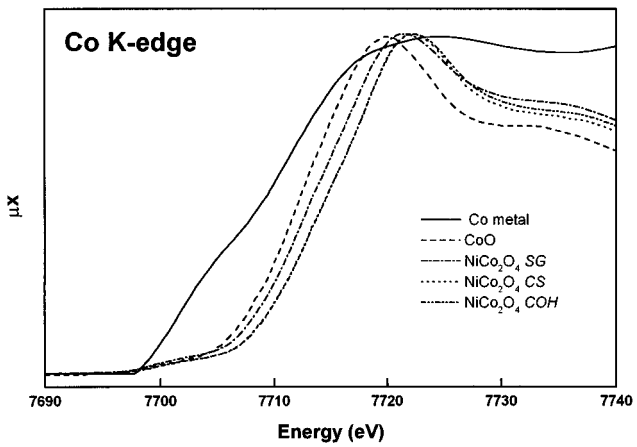

FIG. 3. Co K-edge XANES.

TABLE 6
Final Fitting Parameters Obtained from the Fit of the Co K-Edge EXAFS

Sample	Atom type	Coordination number	Distance (Å)	$2\sigma^2$ (Å^2)
$NiCo_2O_4$ (CS)	O	4	1.89	0.004
	O	2	2.02	0.021
	O	6	2.81	0.001
	Ni	8	3.30	0.019
$NiCo_2O_4$ (SG)	O	3	1.89	0.004
	O	2	2.00	0.038
	O	6	2.82	0.001
	Ni	8	3.31	0.021
$NiCo_2O_4$ (COH)	O	3	1.88	0.002
	O	3	1.98	0.022
	O	6	2.81	0.001
	Ni	8	3.30	0.023

transition of the tetrahedral Co^{2+} ion and that arising from the $1s \rightarrow 4t_{1u}$ transition of the octahedral low-spin Co^{III} ion. According to Lenglet *et al.* (10), tetrahedral Co^{3+} in a high spin state as in garnets may also exist in $NiCo_2O_4$, in which case the corresponding $1s \rightarrow 3d$ transition would also be contributing to the broad pre-edge feature.

The Co K-edge EXAFS of the $NiCo_2O_4$ prepared by different methods were fitted in terms of two Co–O distances accounting for octahedral and tetrahedral occupancies. The fits gave a distance of 1.98–2.02 Å for the tetrahedral Co^{2+}–O length and a distance of 1.88–1.89 Å for the octahedral Co^{III}–O length, similar to that reported by Lenglet *et al.* (10). A third distance at ca. 1.85 Å was also considered to examine the possibility of a third high-spin trivalent cobalt atom in tetrahedral coordination. The quality of the three distances fit did not significantly improve with respect to that of the two distances fit. Thus, we only present here the results corresponding the two distances fit (Table 6 and Fig. 4). We would comment, however, that the measured Co^{2+}/Co^{3+} ratios (0.50, 0.66, and 1.00 for the CS, SG, and COH materials, respectively) require some fraction of high-spin Co^{3+} ions to occupy the tetrahedral sites of the spinel structure to achieve the mass balance on those sites. Since this fraction is small compared to the total amount of Co^{3+} and the tetrahedral Co^{3+}–O distance of 1.85 Å is close to the octahedral Co^{III}–O distance of 1.88 Å, it is not surprising that the fit of the EXAFS data did not improve when the tetrahedral Co^{3+}–O distance was considered. Taken together, the Ni and Co K-edge EXAFS and the XRD results suggest the following approximate cation distributions for the $NiCo_2O_4$ samples made by different methods:

CS: $\{Co^{2+}_{0.65}Co^{3+}_{0.35}\}_{tet}[Ni^{2+}_{0.37}Ni^{3+}_{0.61}Co^{III}_{1}]_{oct}$

SG: $\{Co^{2+}_{0.81}Co^{3+}_{0.19}\}_{tet}[Ni^{2+}_{0.24}Ni^{3+}_{0.75}Co^{III}_{1}]_{oct}$

COH: $\{Co^{2+}_{0.96}Co^{3+}_{0.04}\}_{tet}[Ni^{2+}_{0.14}Ni^{3+}_{0.85}Co^{III}_{1}]_{oct}$.

The lattice parameters calculated from these distributions using the metal–oxygen distances derived from the EXAFS data (8.066 Å, 8.104 Å, and 8.118 Å for the CS, SG, and COH materials, respectively) are very close to the experimental data (Table 1).

TABLE 5
Co K-Edge Positions

Sample	Edge position (eV)	Δ^a (eV)	Edge maximum (eV)
Co	7708.9	—	—
CoO	7712.2	3.3	7720.1
$NiCo_2O_4$ (CS)	7714.5	5.6	7722.4
$NiCo_2O_4$ (SG)	7713.2	4.3	7721.1
$NiCo_2O_4$ (COH)	7714.4	5.5	7722.5

[a]Δ is the energy difference between the position of the edge in the compound and that of Co metal.

3.2. Surface Characterization

The wide scan spectra recorded from the $NiCo_2O_4$ samples prepared by the three different methods showed the expected Co, Ni, O, and C contributions. No peaks which could correspond to carbonate contamination were observed either in the C 1*s* or the O 1*s* spectra (see below). Only in the case of the SG material was a very weak Cl^- signal (BE = 199.0 eV, atomic Cl/O ratio = 0.01) observed.

The interpretation of the Ni 2*p* X-ray photoelectron spectra in oxygenated compounds is rather controversial since, as previously reported (25), conventional fitting methods with Lorentzian–Gaussian functions are unable to

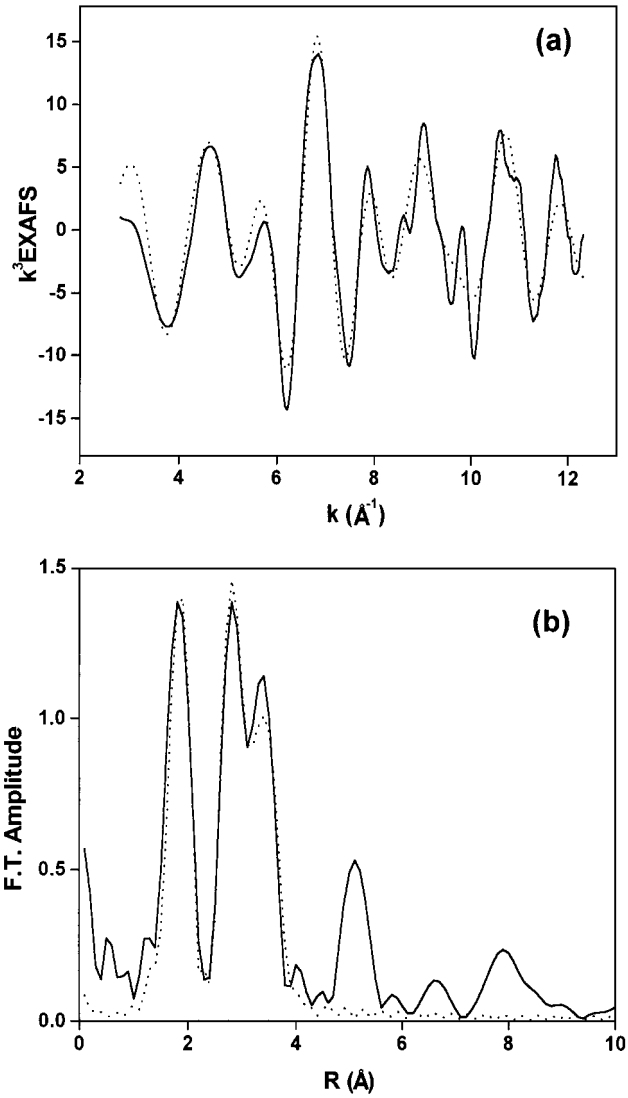

FIG. 4. (a) Co K-edge EXAFS of $NiCo_2O_4$ prepared via the sol–gel method and (b) its corresponding Fourier transform (solid curve, experiment; dashed curve, fitted curve).

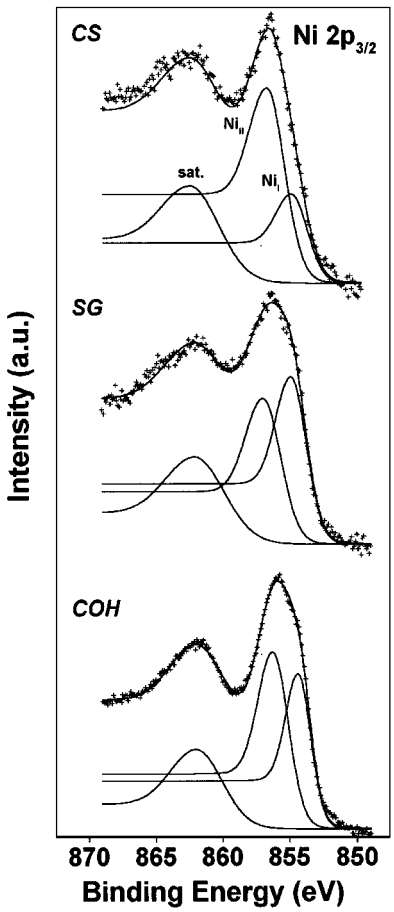

FIG. 5. Ni $2p_{3/2}$ X-ray photoelectron spectra.

distinguish, *a priori*, the number of species present in a sample. Thus, the fitting approach for the Ni $2p_{3/2}$ X-ray photoelectron spectra recorded from the materials synthesized by the three different methods (Fig. 5) cannot be considered unique since, for the same spectrum, different plausible models can yield very reasonable values of χ^2. In the present case, the spectra recorded from the $NiCo_2O_4$ samples were fitted to three components. The line at 854.4 eV (FWHM = 3.3 eV), Ni_I, corresponds to the Ni^{2+} ions located in the octahedral sites of the spinel structure (26, 27) while that at 856.6 eV (FWHM = 3.6 eV), Ni_{II}, is compatible with the presence of Ni^{3+} (28, 29). The 'shake-up" satellite peak centered at 862.0 eV (FWHM = 6.0 eV) contains both Ni^{2+} and Ni^{3+} satellites and has been fitted considering only one broad line. The spectral Ni_I/Ni_{II} area ratios (i.e., Ni^{2+}/Ni^{3+} ratios) obtained from the main lines at 854.4 eV and 856.6 eV vary according to the method of preparation. The Ni^{2+}/Ni^{3+} ratio is highest for the material prepared by sol–gel methods (1.0) and is lowest for the material prepared by thermal decomposition of carbonates (0.4). The Ni^{2+}/Ni^{3+} ratio for the material prepared by decomposition of hydroxides is ca. 0.7.

The Co 2*p* X-ray photoelectron spectra obtained from the materials made by the three different methods were all similar (Fig. 6) and resemble that recorded from Co_3O_4 (30). They were consequently fitted using the same approach (30). The assignment of the different components in the spectra has been given detailed consideration elsewhere (30, 31) and will not be repeated here. All the spectra show components due to Co^{2+} and Co^{3+} with the Co^{2+}/Co^{3+} ratio being 1.7 in all cases.

The O 1*s* spectra recorded from the three $NiCo_2O_4$ materials made by different methods (Fig. 7) contain four oxygen contributions which we have denoted as O1, O2, O3, and O4. Component O1 at 529.2 eV is typical of

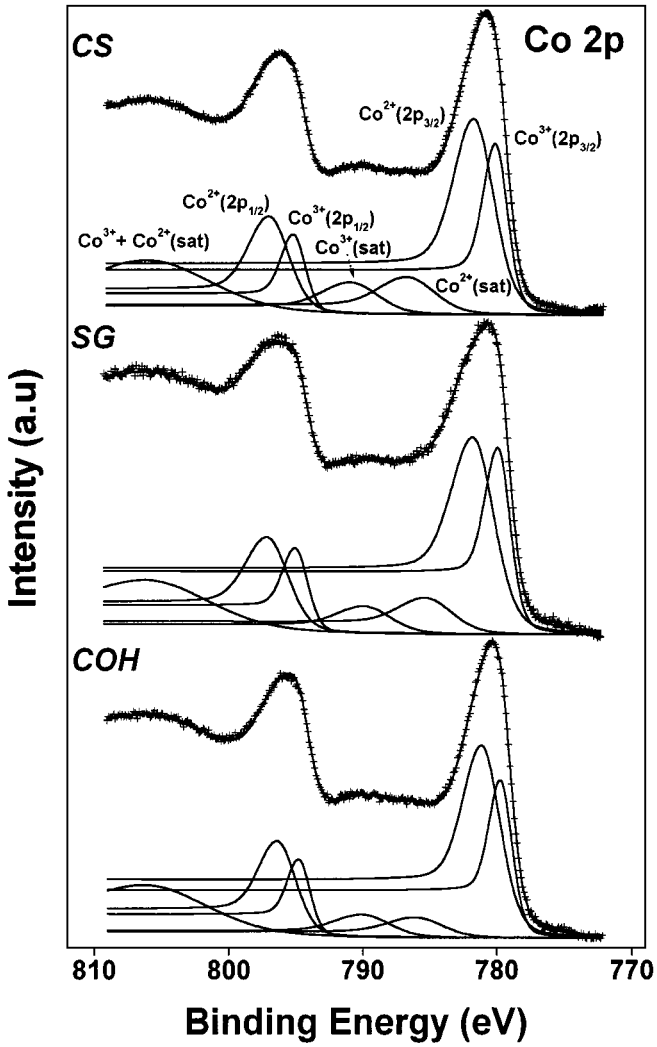

FIG. 6. Co 2*p* X-ray photoelectron spectra.

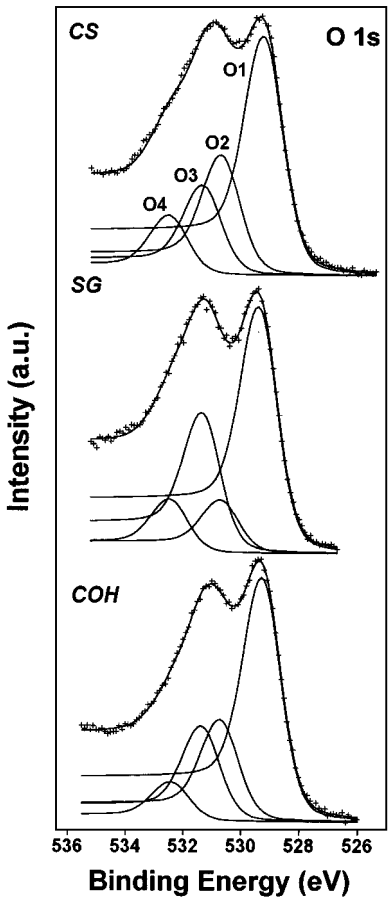

FIG. 7. O 1*s* X-ray photoelectron spectra.

metal–oxygen bonds (32). The component O2 at 530.6 eV is usually associated with oxygen in OH^- groups (32) and the presence of this contribution in the O 1*s* spectra indicates that the surface of the $NiCo_2O_4$ materials is hydroxylated to some extent as a result of either surface oxyhydroxide or the substitution of oxygen atoms at the surface by hydroxyl groups (33). Contribution O3 is located at 531.5 eV and this high binding energy oxygen component has recently been associated with oxygen ions in low coordination at the surface (34). Inspection of Fig. 7 shows that this component is enhanced in the case of the material made by sol–gel methods which scanning electron microscopy has shown to have the lowest particle size (35, 36). Thus, the well-resolved O3 component in the XP spectrum of $NiCo_2O_4$ made by sol–gel methods corresponds to a higher number of defect sites with low oxygen coordination in the material with the smallest particle size. Finally, component O4 can be attributed to multiplicity of physi- and chemisorbed water at and within the surface (32).

The XPS results show significant and clear differences for $NiCo_2O_4$ prepared by different methods (Table 7). The surface Ni^{2+}/Ni^{3+} ratios increase in the order carbonate < hydroxide < sol–gel. The Ni/Co atomic ratios, which should be 0.5 for the stoichiometric compound, show surface enrichment in Ni at the surface of the material prepared by the sol–gel methods (1.16) and a clear depletion of Ni in the surface of the material prepared by thermal decomposition of carbonates (0.32). The sum of the Co/O and Ni/O atomic ratios is close to 0.75, which corresponds to the metal/O atomic ratio of the bulk where the stoichiometric Ni/Co ratio has to be 0.5. Presumibly, charge balance when $Ni/Co \neq 0.5$ is achieved either by changing the oxidation states of Ni and/or Co surface cations, or by substituting surface O^{2-} by hydroxyl groups. The results show that the surface properties of $NiCo_2O_4$ depend on the method of preparation.

The results reported have shown that different preparation methods lead to materials having similar nominal

TABLE 7
Atomic Ratios Obtained from the XPS Spectra

Synthesis procedure	Ni/Co	Ni/O	Co/O
$NiCo_2O_4$ (CS)	0.32	0.19	0.63
$NiCo_2O_4$ (SG)	1.16	0.43	0.32
$NiCo_2O_4$ (COH)	0.93	0.35	0.40

compositions but different bulk and surface cation distributions. An immediate consequence of this is that the physicochemical properties of the materials should vary according to the type of synthesis method employed. We have observed (37) that some electrochemical properties of $NiCo_2O_4$, such as the electrochemical insertion of lithium, the open circuit voltage value, or the discharge curve when it is used as an electrode for lithium batteries, are noticeably different in the material made via thermal decomposition of carbonates than in the material made by sol–gel methods. Although very preliminary, the results reported here suggest that the properties of a material can be tailored for a particular application by selecting an appropriate synthesis method.

4. CONCLUSIONS

(1) Different synthesis methods yield $NiCo_2O_4$ with similar nominal composition and spinel structure but with significantly different distributions of cation oxidation states.

(2) The surface composition of $NiCo_2O_4$ depends on the method of preparation. The oxidation states of the surface cations do not resemble the distributions in the bulk.

ACKNOWLEDGMENTS

The authors acknowledge financial support from he Chilean CONICYT under Projects 7990026 and 1990951 (Cooperación Internacional-Fondecyt), the Spanish Dirección General de Enseñanza Superior for the award of travel grants (J.F.M. and M.G.) to Daresbury Laboratory, and the EPSRC for the award of beamtime at Daresbury Laboratory.

REFERENCES

1. J. Haenen, W. Visscher, and E. Barendrecht, *J. Elecetroanal. Chem.* **208,** 273 (1986).
2. B. Marsan, N. Fradette, and G. Beaudoin, *J. Electrochem. Soc.* **139,** 139 (1992).
3. M. R. Gennero de Chialvo and A. C. Chialvo, *Electrochim. Acta* **38,** 2247 (1993).
4. R. N. Singh, J. F. Koenig, G. Poillerat, and P. Chartier, *J. Electroanal. Chem.* **314,** 241 (1991).
5. N. Heller-Ling, M. Prestat, J. L. Gautier, J. F. Koenig, G. Poillerat, and P. Chartier, *Electrochim. Acta* **42,** 197 (1997).
6. P. Cox and D. Pletcher, *J. Appl. Electrochem.* **20,** 549 (1990).
7. S. Trasatti, *in* "Transition Metal Oxides: Versatile Materials for Electrocatalysis in Electrochemistry of Novel Materials," (J. Lipkowski and P. N. Ross, Eds.), Chap. 5. VCH, Weinheim/New York, 1994 (and references therein cited).
8. L. A. de Faria, M. Prestat, J. F. Koenig, P. Chartier, and S. Trasatti, *Electrochim. Acta* **44,** 1481 (1998).
9. O. Knop, K. I. G. Reid, Y. Sutarno, and Y. Nakamurå, *Can. J. Chem.* **46,** 3463 (1968).
10. M. Lenglet, R. Guillamet, J. Dürr, D. Gryffroy, and R. E. Vandenberghe, *Solid State Commun.* **74,** 1035 (1990).
11. M. R. Tarasevich and B. N. Efremov, Properties of spinel-type oxide electrodes, in "Electrodes of Coinductive Metallic Oxides," (S. Trasatti, Ed.), Part A, p. 223. Elsevier, Amsterdam, 1980.
12. M. El Baydi, G. Poillerat, J. L. Rehspringer, J. L. Gautier, J. F. Koenig, and P. Chartier, *J. Solid State Chem.* **109,** 281 (1994).
13. J. Ponce, E. Ríos, J. L. Rehspringer, G. Poillerat, P. Chartier, and J. L. Gautier, *J. Solid State Chem.* **145,** 23 (1999).
14. P. Ravindranathan, G. V. Manesh, and K. C. Patil, *J. Solid State Chem.* **66,** 20 (1970).
15. N. Yamamoto, S. Higasi, S. Kawano, and N. Achiwa, *J. Mater. Sci. Lett.* **2,** 525 (1983).
16. N. Binsted, S. Gurman, and J. Campbell, Laboratory EXCURV90 program, Daresbury Laboratory, 1990.
17. S. J. Gurman, N. Binsted, and I. Ross, *J. Phys. C* **17,** 143 (1984).
18. J. B. Pendry, "Low Energy Electron Diffraction." Academic Press, New York, 1974.
19. S. Sasaki, K. Fujino, and Y. Takeuchi, *Proc. Jpn. Acad.* **55,** 43 (1979).
20. X. Liu and C. T. Prewitt, *Phys. Chem. Miner.* **17,** 168 (1990).
21. R. W. Joyner, K. J. Martin, and A. Meehan, *J. Phys. C* **20,** 4005 (1987).
22. P. M. A. Sherwood, Data Analysis in X-ray Photoelectron Spectroscopy, *in* "Practical Surface Analysis," (D. Briggs and M. P. Seah, Eds.), 2nd edn., Vol. 1: Auger and X-ray Photoelectron Spectroscopy. Wiley, Chichester, 1990.
23. C. D. Wagner, L. E. Davis, M. V. Zeller, J. A. Taylor, R. M. Raymond, and L. H. Gale, *Surf. Interface Anal.* **3,** 211 (1981).
24. W. E. O'Grady, K. I. Pandya, K. E. Swider, and D. A. Corrigan, *J. Electrochem. Soc.* **143,** 1613 (1996).
25. A. R. Gonzalez-Elipe, J. P. Holgado, R. Alvarez, and G. Munuera, *J. Phys. Chem.* **96,** 3080 (1992).
26. M. Lenglet, A. d'Huysser, J. P. Bonelle, J. Dürr, and C. K. Jørgesen, *Chem. Phys. Lett.* **136,** 478 (1987).
27. M. Lenglet, A. d'Huysser, J. Arsène, J. P. Bonelle, and C. K. Jørgesen, *J. Phys. C*: *Solid State Phys.* **19,** L363–L368 (1986).
28. N. S. McIntyre and M. G. Cook, *Anal. Chem.* **47,** 2208 (1975).
29. K. S. Kim and N. Winograd, *Surf. Sci.* **43,** 625 (1974).
30. J. L. Gautier, E. Rios, and J. F. Marco, *Bol. Soc. Chil. Quim.* **43,** 447 (1998).
31. J. L. Gautier, E. Rios, M. Gracia, J. F. Marco, and J. R. Gancedo, *Thin Solid Films* **311,** 51 (1997).
32. T. Choudhury, S. O. Saied, J. L. Sullivan, and A. M. Abbot, *J. Phys. D*: *Appl. Phys.* **22,** 1185 (1989).
33. Yu. E. Roginskaya, O. V. Morozova, E. N. Lubnin, Yu. E. Ulitina, G. V. Lopukhova, and S. Trasatti, *Langmuir* **13,** 4621 (1997).
34. V. M. Jiménez, A. Fernández, J. P. Espinós, and A. R. González-Elipe, *J. Electron Spectrosc. Relat. Phenom.* **71,** 61 (1995).
35. M. El Baydi, S. K. Tiwari, R. N. Singh, J. L. Rehspringer, P. Chartier, J. F. Koenig, and G. Poillerat, *J. Solid State Chem.* **116,** 157 (1995).
36. C. A. Ramos, Thesis, USACH-Santiago-Chile, 1997.
37. J. L. Gautier, C. Ramos, E. Meza, J. R. Gancedo, and J. F. Marco, Innovative Materials in Advanced Energy Technologies, *in* "Proceedings of the *9th Cimtec-World Forum on New Materials*," (P. Vincenzini, Ed.), Advances in Science and Technology 24, p. 141. Techna Srl., Faenza, Italy, 1999.